p-ISSN 2089 – 0133 e-ISSN 2477-6416
URL : https://jurnal.uns.ac.id/ijap/article/view/93369
Indonesian Journal of Applied Physics (IJAP) Vol. 14 No. 2 page 417
DOI : https://doi.org/10.13057/ijap.v14i2.93369

THE IDENTIFICATION OF FAULTS USING MAGNETIC METHOD IN KULONPROGO, YOGYAKARTA, INDONESIA

Sorja Koesuma[1], Sehah[2], Choirul Singgih Munandar[1]
[1]Department of Physics, Sebelas Maret University, Surakarta, Indonesia
[2]Department of Physics, Jenderal Soedirman University, Purwokerto, Indonesia
[*]sorja@staff.uns.ac.id

Received 13-09-2024, Revised 12-10-2024, Accepted 22-10-2024,
Available Online 22-10-2024, Published Regularly October 2024

ABSTRACT

The aims of this study to identify faults and identify subsurface lithology using magnetic anomaly data in the Kulonprogo. In the acquisition was carried out using a Proton Procession Magnetometer (PPM) Geotron G5 with 62 measurement points and a distance of ±1 km between point. Measurements were made on Kebobutak (Tmok), Aluvium (Qa), Andesit (a), and Sentolo (Tmps) formations. The total magnetic field data processing is done with several correction, namely diurnal correction, IGRF, reduce to equator, upward continuation at an altitude of 2000 m, and reduce to pole, and 2D modelling using the forward modelling method. The result of the analysis obtained magnetic field anomaly values in the range of values -400 to 950 nT. The 2D modelling shows that the research area is composed of 4 dominating rock types, namely andesite rock with a susceptibility value of 94 x 10^{-3}, andesite breccia rock with a susceptibility value of 29 x 10^{-3}, clay rock with a susceptibility value of 0,013 x 10^{-3}, and sandstone with a susceptibility value of 5 x 10^{-3}. The identification result shows the existence of faults line on Mount Watuaglik, Mount Kamal, and Mount Bodag.

Keywords: Magnetic method; Faults; Forward Modelling

Cite this as: Koesuma, S., Sehah., & Munandar, C. S. 2024. The Identification of Faults Using Magnetic Method in Kulonprogo, Yogyakarta, Indonesia. *IJAP: Indonesian Journal of Applied Physics, 14*(2), 417-427. doi: https://doi.org/10.13057/ijap.v14i2.93369

INTRODUCTION

Indonesia is an area that is very prone to natural disasters, both geological and meteorological. There are three earth tectonic plates that meet in the Indonesian area, namely the Eurasian plate, the Pacific plate, and the Indo-Australian plate [1]. From this, Indonesia is one of the countries in the world that often experiences earthquake disasters, both volcanic and tectonic earthquakes.

The Yogyakarta is one of the most earthquake-prone areas in Indonesia. This is because the Yogyakarta area is located in the subduction zone of the Indo-Australian Plate to the Eurasian Plate in the Indian Ocean south of Java Island. From its location, the Yogyakarta area is the most tectonically active area in Indonesia, especially in the Kulonprogo Regency area. One of the tectonic activities occurred in Yogyakarta on 27 May 2006 which caused a large earthquake with a magnitude of 6.3 Mw in the early morning local time [2]. According to geology, Central Java is divided into six physiographic zones, namely Quaternary Volcanoes, North Java Alluvial Plain, North Serayu Anticlinorium, Domes and Mountains in the Central Depression Zone, Central Depression Zone and Southern Mountains. Based on the division of physiographic zones, the research area is part of the Central Depression Zone. The research area to the north is in the Central Depression zone which consists of the Sentolo Formation, Kebobutak Formation, Jonggrangan Formation and Andesite Intrusion [3].

This research was conducted in Kulonprogo Regency, Yogyakarta. This area was chosen because of the news of this area becoming an aerotropolis. Aerotropolis is an independent urban development area of an airport that functions as an economic centre, has functional linkages and an integrated and centralised infrastructure network system or airport city [4]. Based on the results of previous research presented by Zamroni et al. (2021) [5], the map shows faults on the east and west sides of the Yogyakarta International Airport which extend north to the mountains. According to Nurul et al. (2018) [6], there are several fault lines in the villages of Kalirejo, Kokap which are strike slip faults and normal faults. And according to Syafri et al (2013) [7], there is a horizontal fault in the Wates area that extends to the north with the dominating rocks being alluvial and andesite.

Data collection using geomagnetic methods is based on the measurement of the earth's magnetic field anomalies that are influenced by contrasting differences in the level of magnetism (susceptibility) or the ability of rocks to pass fluids (permeability) magnetic body traps from the surrounding area. Magnetometer is a tool used in measuring the earth's magnetic field anomaly [8]. 2D modelling of reduce to pole local anomaly data in this study was carried out using the forward modelling method. Forward modelling is an indirect modelling of data or it can be said to estimate the magnetic susceptibility value of subsurface rocks by making a model of anomaly objects first [9].

METHOD

Magnetic Force

Magnetic force has the same concept as Coulomb's Law which states that the amount of force between two magnetically charged objects will be inversely proportional to the square of the distance between the two objects. Magnetic force is a force that attracts or repels each other between the two magnetic poles separated by a distance r and produces a magnetic force F. Telford (1990) [10] states that the underlying Coulomb force of the geomagnetic method between the two sides of the magnetic poles m_1 and m_2 (emu) is the distance (metres) which can be calculated as follows:

$$\vec{F} = \frac{m_1 m_2}{\mu_0 r^2}\hat{r} \qquad (1)$$

where $\vec{F}$ is the magnetic force, m_1 and m_2 are the polar charges, $\hat{r}$ is the distance between the poles, and μ_o is the permeability of the magnetic medium.

Diurnal Correction

Total magnetic field anomaly is the result after diurnal correction and IGRF. Diurnal correction is an error in the value of the earth's magnetic field caused by differences in solar radiation and time of day differences. If the value of the daily variation is negative (-), then the diurnal correction is done by adding the value of the daily variation recorded at a certain time to the magnetic field data to be corrected. This applies vice versa, if the daily variation is positive (+) then the correction can be done by subtracting the daily variance value recorded at a certain time from the magnetic field data to be corrected which can be calculated as follows [11]:

$$\Delta H_h = \left(\frac{t_n - t_a}{t_{ak} - t_a}\right)(H_{ak} - H_a) \qquad (2)$$

where H_h is the daily magnetic field value, t_n is the nth data time, t_a is the time at the beginning of the data, t_{ak} is the time at the end of the data, H_a is the magnetic field intensity at the beginning, and H_{ak} is the magnetic field intensity at the end.

IGRF Correction

Data obtained from the field is raw data that is still influenced by three factors, namely the earth's main magnetic field (main field), external magnetic field (external field) and anomaly magnetic field (anomaly field). The main magnetic field value is the International Geomagnetic Reference Field (IGRF) value. This value can be accessed through https://www.bmkg.go.id/geofisika-potensial/kalkulator-magnet-bumi.bmkg. The contribution data from the main magnetic field should be removed by IGRF correction in a way [12]:

$$\Delta H = H_{diurnal} - H_{IGRF} \quad (3)$$

$$H_{diurnal} = H_{total} \pm V_{diurnal} \quad (4)$$

where ΔH is the total magnetic field anomaly, $H_{diurnal}$ is the diurnal magnetic field strength, H_{IGRF} is the Earth's main magnetic field, H_{total} is the measured magnetic field strength, and $V_{dirunal}$ is the diurnal variance.

Reduce to Equator

The total anomaly map is still difficult to interpret so that transformations are needed to show the position of the research object. Reduction to equator is done to facilitate the processing of magnetic anomaly data, anomaly data that is still distributed on topographic surfaces (not flat) is reduced to a flat field. This transformation process is absolutely necessary because the next processing requires the input of magnetic field anomalies that are distributed on a flat plane, this process also needs to be done if the height of the data collection point has a significant difference or fluctuation. This reduction uses the Taylor approach which can be written as follows [13]:

$$\Delta H_{(x,y,zo)} = \Delta H_{(x,y,z)} - \Sigma_{n=1}^{n} \frac{z-z0}{n!} \frac{\partial^n}{\partial x^n} \Delta H_{(x,y,zo)} \quad (5)$$

Upward Continuation

The process of separating regional anomalies and residual anomalies in this research uses the *upward continuation* method. Upward continuation is the transition of potential field deta originating from a flat field to another higher flat field. The principle of this transformation is a high pass filter by passing a higher signal, this process is carried out in stages which is useful for knowing changes in the resulting pattern. The result of this process is a regional anomaly that will be subtracted from the total magnetic anomaly that has been reduced by the flat field with the following equation [14].

$$\Delta H_{local} = \Delta H\ (x,y,z_0) - \Delta H_{reg} \quad (6)$$

Reduce to Pole

Reduction to pole is one of the processes to change the anomaly from dipole to monopole so that this correction can facilitate the interpretation of magnetic data. The basis of using this filter is because there are different values of inclination and declination in each region, so the use of this filter is in order to change the magnetic field in the research location into a magnetic field at the magnetic north pole [15].

Forward Modelling

Forward modelling is modelling done to obtain theoretical values from the results of data acquisition in the field of subsurface model parameters. At this stage (modelling) is done to interpret geophysical data such as magnetic, gravity, and seismic [16]. During the interpretation stage, a model that can obtain results in accordance with field data is sought. So that the results obtained from the model can be close to the actual situation. This modelling is done by trial and error to get the appropriate results between theoretical data and field data, and it is expected to obtain a model that matches the response to the data. In fault identification, Forward modelling is used to predict fault location, fault type and fault length [17].

RESULTS AND DISCUSSION

Kulonprogo has several types of rocks that dominate especially in the research area according to the geological map of Yogyakarta sheet dominated by andesite, breccia, alluvial, and sandstone rocks, as in Figure 1. From this geological map that will be a guideline for 2D modelling and data interpretation.

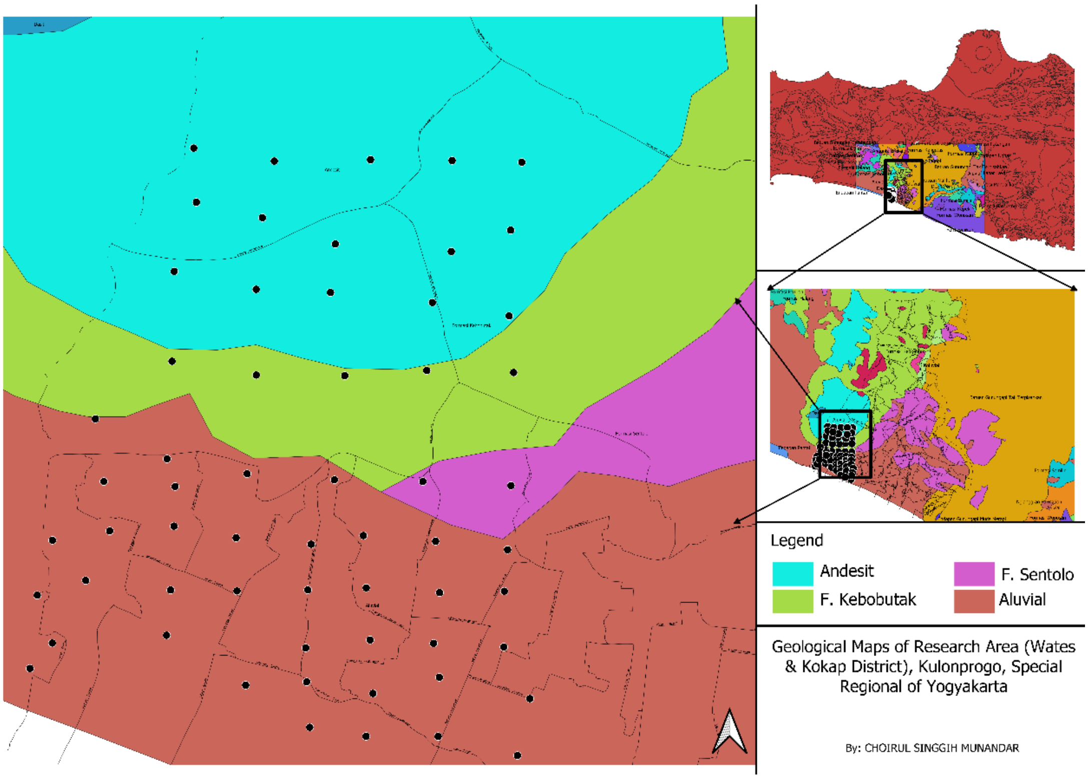

Figure 1. Geological Map of Yogyakarta Sheet [18]

Data processing is carried out to identify faults and determine the subsurface lithology that can be seen from changes in the magnetic field intensity value at the research location. The stage carried out in data processing is to make corrections, the corrections made are diurnal corrections and IGRF corrections. Diurnal corrections are made to eliminate deviations in the value of the earth's magnetic field due to differences in the effects of solar radiation and time differences in one day. While the IGRF correction is done to eliminate the influence of the earth's magnetic field measured along with the magnetic field. The results of the total magnetic field anomaly can be seen in Figure 2.

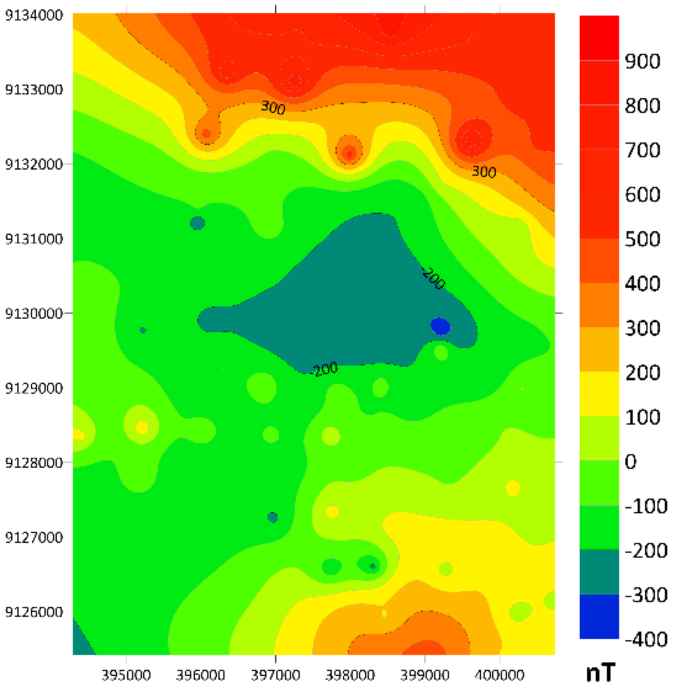

Figure 2. Total Anomaly Magnetic

The total magnetic field anomaly has a range of values from -400 to 950 nT. Low anomaly values are shown in blue with values between -400 to -200 nT. Medium anomaly values are shown in green to yellow with values between -200 to 200 nT. While high anomaly values are indicated by red to purple colours with values between 200 to 950 nT. In general, the closure pattern of magnetic anomaly before and after correction is almost the same, this can be understood because the contribution of the earth's main magnetic field or IGRF to the acquisition data at all measurement points is almost the same. The contribution of the external magnetic field is also very small, so it does not affect the total magnetic anomaly closure pattern significantly [19]. This magnetic field anomaly needs to be processed again to get a local anomaly. The next process is reduce to equator.

Reduce to equator in this study is carried out if the magnetic field anomaly value is at an uneven height or elevation due to data distortion in the total magnetic field anomaly value. This process is absolutely necessary because further processing requires the elevation to be brought to a flat plane. This reduction process uses the Taylor approach. The height taken is 52.4 metres which is the average height of the study.

Figure 3 is the result of the reduce to equator at an average height on topography of 52.4 metres. The total magnetic field anomaly values after being reduced to pole range from -400 to 950 nT. Low anomaly are shown in blue with values ranging from -400 to -200 nT, for medium anomaly are shown in green to yellow with values ranging from -200 to 200 nT, while for high anomalies are shown in red to purple with values ranging from 200 to 950 nT. After this, the next process is to separate the anomalies by lifting up.

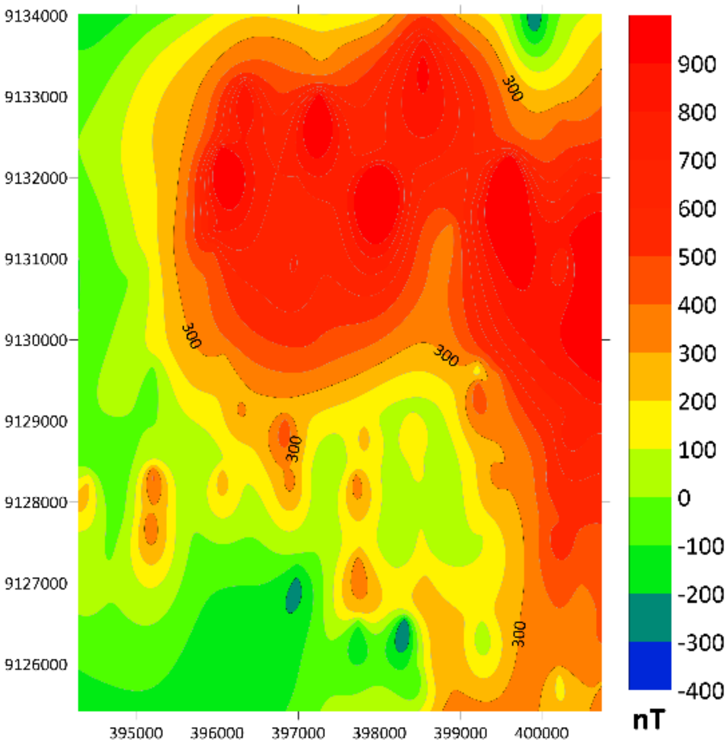

Figure 3. Reduce to Equator

The upward continuation process is used for anomaly separation which is a process to separate regional anomalies and residual anomalies. Residual anomalies are anomalies that are closer to the surface or can be called local anomaly, while regional anomaly are anomaly that are deeper than residual anomaly. The was taken at an altitude of 2000 metres. This is with the consideration that at this height the influence of the residual anomaly has disappeared and the contours have converged.

Figure 4 The change in the smoothness of the clossure at each elevation change is caused by the disappearance of the influence of objects in the shallow depths, therefore, it is necessary to limit the elevation to anticipate the disappearance of the research target. The higher uplift causes the fault line as the target to become less obvious.

The range of values changed to 140 to 520 nT. The distribution of high to low values is increasingly evident with high values scattered in the north of the study and experiencing changes in the lower spread in the south of the study area. In the upward continuity process, regional anomaly are obtained which are then corrected or reduced with total magnetic anomaly data that reduce to equator. The result of the correction is local magnetic anomaly data distributed on a reduce to equator with the same height as the total magnetic anomaly data.

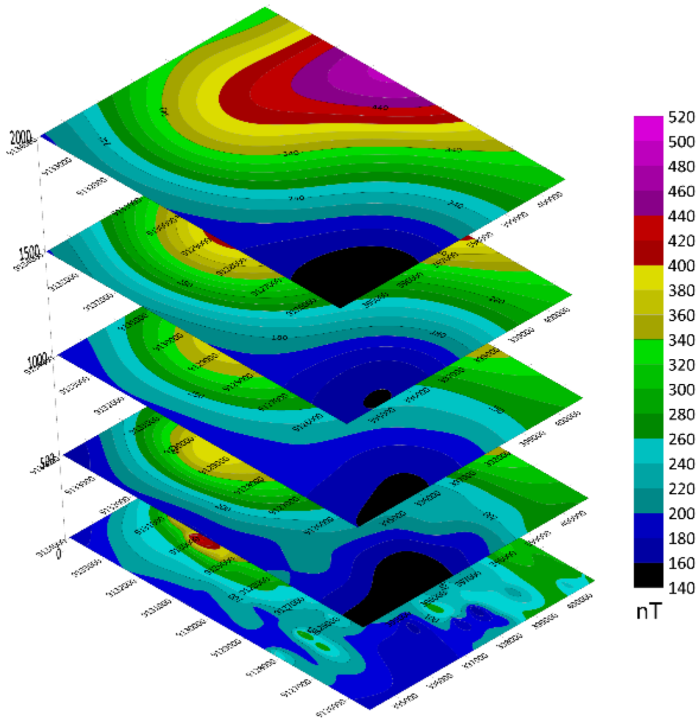

Figure 4. Upward Continuition 2000 m high

In Figure 5 the distribution of local anomaly values ranges from -400 to 950 nT. Low anomaly are shown in blue with values ranging from -400 to -200 nT, for medium anomaly shown in green to yellow with values ranging from -200 to 200 nT, while for high anomaly shown in red to purple with values ranging from 200 to 950 nT.

The last step is done because the previous process obtained local anomalies and regional anomalies, both of which still have dipole or two poles. Anomalies that are dipole in nature will complicate interpretation so it is necessary to uniform the polar direction of the anomaly. One of the ways that can be uniformed is the reduction process to the pole, this process is done by changing the direction of the anomaly from the anomaly towards the north of the earth by changing the declination and inclination values to 0^o and 90^o, respectively.

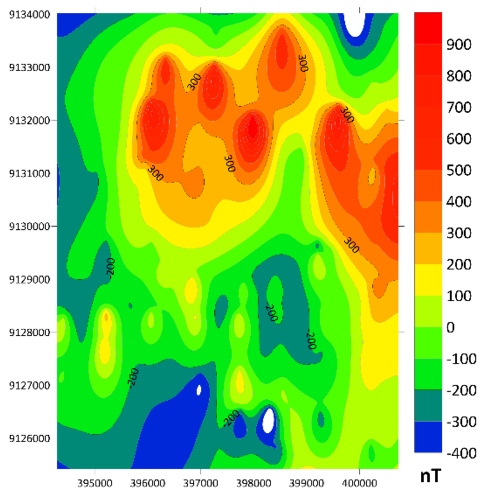

Figure 5. Residual Anomaly Map

In Figure 6, there is a significant change from local anomalies to reduce to pole with a range of -1400 to 1450 nT. Low anomalies are shown in blue with values ranging from -1400 to -200 nT, for medium anomalies are shown in green to yellow with values ranging from -200 to 200 nT, while high anomalies are shown in orange to purple with values ranging from 200 to 1450 nT. Early indications of faulting can be seen in this process where the map shows a sudden decrease in value.

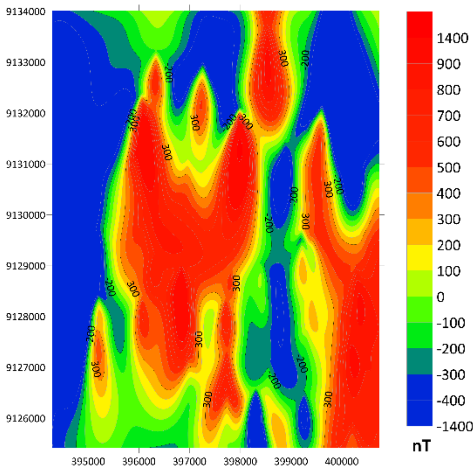

Figure 6. Reduce to Pole

The parameters required in this process are rock susceptibility, position, inclination, and declination. Figure 7 shows the incisions used in the 2D modelling process. Modelling was carried out on the residual anomaly map by making 3 incisions that cut the fault according to the geological map sheet Yogyakarta.

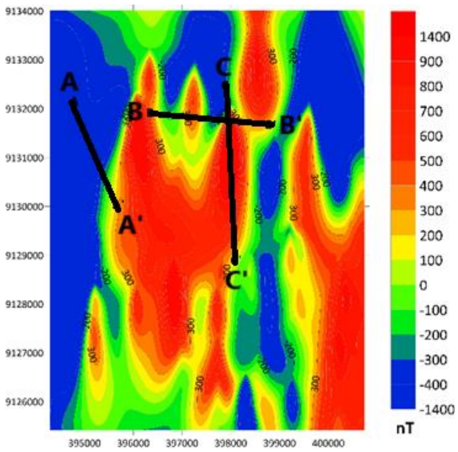

Figure 7. Trajectory Line for Cross-Section Modelling

The next step is 2D modelling using the forward modelling method. The modelling results of the AA' incision can be seen in Figure 8. there are three dominant rock types with an incision length of ± 2415 metres shown in Figure 4.13. The uppermost rock layer has a susceptibility value ranging from 0,013 x 10^{-3} SI with a layer depth of ±0 to 523 metres from the surface with varying thickness, the first rock layer is estimated to be top soil dominated by clay. The second layer has a susceptibility ranging from 29 x 10^{-3} SI with a layer depth of ±294 to 838 metres from the surface with varying thickness, the second rock layer is thought to be dominated by andesite breccia rocks. While the third layer has a susceptibility ranging from 94 x 10^{-3} SI with a layer depth of ± 619 to 900 metres from the surface with varying thickness, the third rock layer is thought to be dominated by andesite rocks. The existence of the suspected fault according to the modelling results of the AA' incision is found at a distance of ±828 metres from point A. Based on the modeling line A-A' there are no folds

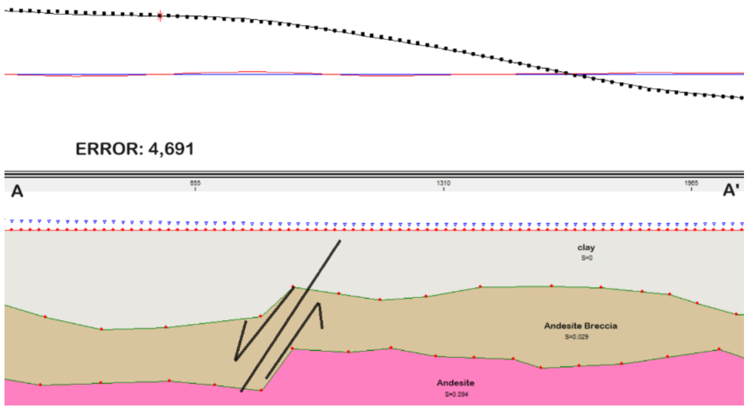

Figure 8. Cross-Section of the Line AA'

There are three dominant rock types with an incision length of ±3002 metres as shown in Figure 9. The uppermost rock layer has a susceptibility value ranging from 0,013 x 10^{-3} SI with a layer depth of ±0 to 596 metres from the surface with varying thickness, the first rock layer is estimated to be top soil dominated by clay. The second layer has a susceptibility value ranging from 29 x 10^{-3} SI with a layer depth of ±27 to 852 metres from the surface with varying thickness, the second rock layer is thought to be dominated by andesite breccia rocks. While the third layer has a susceptibility value of 94 x 10^{-3} SI with a layer depth starting at ±248 metres from the surface with varying thickness, the third rock layer is thought to be dominated by andesite rocks. The existence of the suspected fault according to the modelling result of the BB' incision is found at a distance of ±1469 meters from point B. Based on the modeling line B-B' there are no folds

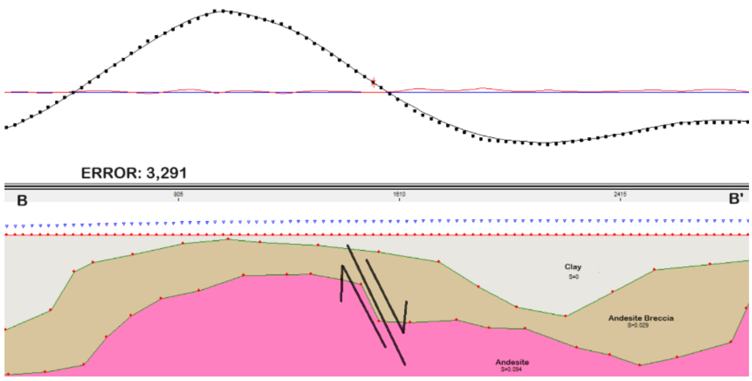

Figure 9. Cross-Section of the Line BB'

The results of the CC' incision modelling can be seen in Figure 10. there are four dominant rock types with an incision length of ±4277 metres shown in Figure 10. The uppermost rock layer has a susceptibility value ranging from 0,013 x 10^{-3} SI with a layer thickness of ±0 to 373 metres from the surface with varying thickness, the first rock layer is estimated to be top soil dominated by clay. The second layer has a susceptibility value ranging from 29 x 10^{-3} SI with a layer thickness of ±90 to 883 metres from the surface with varying thickness, the second rock layer is estimated to be dominated by andesite rock. The third layer has a susceptibility value ranging from 5 x 10^{-3} SI with a layer thickness of ±176 to 337 metres with varying thickness, the third layer is thought to be dominated by sandstone. While the fourth layer has a susceptibility value ranging from 94 x 10^{-3} SI with a layer depth starting from ±392 metres from the surface with varying thickness, the fourth layer is estimated to be dominated by andesite rocks. Based on the modeling line C-C' there are no folds nor faults.

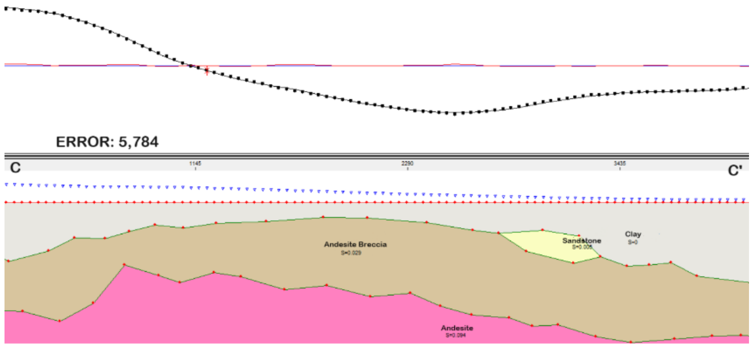

Figure 10. Cross-Section of the Line CC’

CONCLUSION

The conclusion of this research is that based on the 2D modelling results and validation results from the geological map of Yogyakarta sheet, it is known that the fault line is located on Mount Watuaglik, Mount Bodag, and Mount Kamal. The type of fault identified from the modelling results is a normal fault and the subsurface lithology in the study area is dominated by rocks with different susceptibility values, namely clay with a susceptibility value of 0.013 x 10^{-3} SI, andesite breccia rock with a susceptibility value of 29 x 10^{-3} SI, sandstone with a susceptibility value of 5 x 10^{-3} SI, and andesite rock with a susceptibility value of 94 x 10^{-3} SI.

REFERENCES

1 Fuady, M., Munadi, R., & Fuady, M. A. K. 2021. Disaster mitigation in Indonesia: between plans and reality. In *IOP Conference Series: Materials Science and Engineering*, 1087(1), IOP Publishing.

2 Pohan, A, F., Sismanto, S., Nurcahya, B, E., Lewerissa, R., Koesuma, S., Saputro, S, P., & Adhi, M, A. 2023. Utilization and Modelling of Satellite Gravity Data for Geohazard Assessment in the Yogyakarta Area of Java Island, Indonesia. *Kuwait Journal of Science*, 50(4), 499-511.

3 Kusumawati, N. A., Putra, I. D., Wijaya, I. G. N. K., & Indrawan, I. 2018. Integrated remote sensing and geological observation in identifying landslide triggering factors: A case study of landslide hazard of Hargotirto subdistrict, Kulon Progo, DI Yogyakarta. In *AIP Conference Proceedings*, 1987(1), AIP Publishing.

4 Hakim, F. N. 2021. Social Changes Affected by the Development of Yogyakarta International Airport (YIA). In *Proceedings of International Conference on Communication Science*, 1(1), 24-28.

5 Zamroni, A., Sugarbo, O., Trisnaning, P. T., Sagala, S. T., & Putra, A. S. 2021. Geochemical approach for seawater intrusion assessment in the area around Yogyakarta International Airport, Indonesia. *The Iraqi Geological Journal*, 1-11.

6 Nurul, A., Kunang, A., Khoiruddin, A., Nathania, B., Tirani, D., Diofano, E., ... & Delva, Z. 2018. Mineral Prospect Identification Using Inducedpolarization And Very Low Frequency-EM Methods At Sangon, Kalirejo Village, Kokap Sub-District, Kulonprogo Regency, Special Region Of Yogyakarta, Indonesia. Jurnal Fisika Indonesia, 22(3), 1-12.

7 Syafri, I., Budiadi, E., & Sudradjat, A. 2013. Geotectonic Configuration of Kulon Progo Area, Yogyakarta. *Indonesian Journal on Geoscience*, *8*(4), 185-190.

8 Yusof, K. A., Abdullah, M., Hamid, N. S. A., Ahadi, S., & Ghamry, E. 2021. Statistical global investigation of pre-earthquake anomalous geomagnetic diurnal variation using superposed epoch analysis. *IEEE Transactions on Geoscience and Remote Sensing*, *60*, 1-13.

9 Nafian, M., Permana, N. R., Anjani, A., Gunawan, B., & Sanjaya, L. A. 2021. Identification 2D Modelling of Subsurface Structure Geothermal Prospect Area by Gravity Method: Case Study in Tanuhi, South Kalimantan. In *Journal of Physics: Conference Series*, 2019(1), p. 012081. IOP Publishing.

10 Telford, W. M., Geldart, L. P., & Sheriff, R. E. 1990. *Applied geophysics*. Cambridge university press.

11 Maubana, W. M., Maryanto, S., Utami, I. W., & Nadir, A. (2019). Reservoir magnetic anomaly at geothermal area of mount Pandan, East Java, Indonesia. *Int. J. Renew. Energy Res*, *9*(2), 887-892.

12 Permana, N. R., Gunawan, B., Primastika, A. A., Shafa, D., Fadrian, D. F., & Zani, F. R. (2022). Identification of alteration zone and gold mineralization based on magnetic anomaly and 3D model of geomagnetic satellite data inversion of Mount Pongkor Area, West Java. *Journal of Natural Sciences and Mathematics Research*, *8*(2), 94-102.

13 Blackley, D. M., & Follain, J. R. 1996. In search of empirical evidence that links rent and user cost. *Regional Science and Urban Economics*, *26*(3-4), 409-431.

14 Sehah, U. N. P., Raharjo, S. A., & Prasetya, R. I. TWO-DIMENSIONAL MODELING OF MAGNETIC ANOMALY DATA REDUCED TO THE POLES IN THE ANDESITIC PROSPECT AREA OF THE SOUTHEAST SLOPE OF SLAMET VOLCANO, INDONESIA.

15 Baranov, V., & Naudy, H. 1964. Numerical calculation of the formula of reduction to the magnetic pole. *Geophysics*, *29*(1), 67-79.

16 Abudeif, A. M., Ali, M. A., & Mohammed, M. A. 2023. Subsurface Structure Detection Using Geomagnetic Data Approach in Wadi Araba area, Gulf of Suez, Egypt. *Sohag Journal of Sciences*, *8*(3), 337-346.

17 Mosbahi, H., Jrad, A., Dhaoui, M., Azaiez, H., & Montacer, M. 2023. Constrained 3D gravity modelling of a multilayered aquifer system in an arid region: Case of Sebkhat El Bhira basin (Central Tunisia). *Journal of Applied Geophysics*, *210*, 104950.

18 Rahardjo, W., Sukndarrumidi, & Rosidi, H. M. D, 1995, Center for Geological Research and Develompment, Bandung.

19 Sehah, M., Raharjo, S. A., & Risyad, A. 2020. A Geophysical Survey with Magnetic Method for Interpretation of Iron Ore Deposits in the Eastern Nusawungu Coastal, Cilacap Regency, Central Java, Indonesia. *Journal of Geoscience, Engineering, Environment, and Technology*, *5*(1), 37-44.